Entropic characterization of the coil-stretch transition of polymers in random flows

F. Sultanov,[1,5] M. Sultanova,[1,5] G. Falkovich,[1,2] V. Lebedev,[1] Y. Liu,[3] and V. Steinberg[2,4]
[1]*Landau Institute for Theoretical Physics, Moscow region 142432, Russia*
[2]*Weizmann Institute of Science, 76100 Rehovot, Israel*
[3]*Changchun Institute of Applied Chemistry, Changchun 130022, China*
[4]*The Racah Institute of Physics, Hebrew University, Jerusalem 91904, Israel*
[5]*Institute of Solid State Physics, Moscow region 142432, Russia*

(Received 10 November 2020; revised 29 January 2021; accepted 24 February 2021; published 17 March 2021)

Polymer molecules in a flow undergo a coil-stretch phase transition on an increase of the velocity gradients. Model-independent identification and characterization of the transition in a random flow has been lacking so far. Here we suggest to use the entropy of the extension statistics as a proper measure due to strong fluctuations around the transition. We measure experimentally the entropy as a function of the local Weisenberg number and show that it has a maximum, which identifies and quantifies the transition. We compare the new approach with the traditional one based on the theory using either linear Oldroyd-B or nonlinear finite extensible nonlinear elastic polymer models.

DOI: 10.1103/PhysRevE.103.033107

I. INTRODUCTION

Quantitative description of the stretching statistics of polymer molecules in flows is an outstanding problem directly related to wide classes of phenomena from microfluidics to turbulent drag reduction. In this regard, the most important and spectacular statistical phenomenon is the coil-stretch transition: When the product of the velocity gradient and the molecular relaxation time (called the Weissenberg number, Wi) exceeds a certain value, the most probable conformation changes from a coil to a strongly stretched molecule [1].

It pays to distinguish transitions in two types of flow: Steady and random. In a steady purely elongational flow above the critical elongation rate $\dot{\epsilon}$, a polymer coil extends up to almost fully stretched state. The balance between the stretching drag force and the entropic restoring force gives the transition threshold $\mathrm{Wi}_c^{\mathrm{elong}} = \dot{\epsilon}\lambda = 1/2$, where λ is the longest polymer relaxation time [1]. It is then expected that the stretching is negligible at $\mathrm{Wi}^{\mathrm{elong}} < 1/2$, while at $\mathrm{Wi}^{\mathrm{elong}} > 1/2$ it extends abruptly all the way to the maximal extension (determined by the finite extensibility and the conformation-dependent drag [2,3]).

For not very long molecules, the transition was identified experimentally for λ-DNA [4] and numerically for T4DNA [5] by a sharp increase of the steady-state mean polymer extension at $\mathrm{Wi}_c^{\mathrm{elong}} \approx 0.4$, somewhat different from the theoretical value. It also is noteworthy that there exists a strong dispersion of the rate of polymer stretching for individual molecules in identical flows, coined *molecular individualism* [6]. It is caused by the thermal fluctuations of the coil size and shape, amplified by the exponential separation and the heterogeneity in unraveling rates of different conformations: Different polymers feel quite different stretching rates [7]. Similar behavior was found in linear mixed flows [8,9]. For very long molecules (DNA with polymer length $L = 1.3$ mm), the transition in the elongation flow is not continuous but hysteretic in the range of $\mathrm{Wi}_c^{\mathrm{elong}} \approx 0.4$–$0.5$ [2,10–12].

Apart from the mean extension, another way to characterize the transition in elongation flow is to determine the polymer relaxation time to steady state versus $\mathrm{Wi}^{\mathrm{elong}}$, as suggested in Refs. [13,14] using the finite extensible nonlinear elastic (FENE) dumbbell model with conformation-dependent drag. The transition occurs around $\mathrm{Wi}_c^{\mathrm{elong}} \simeq 0.5$, with the exact value determined by the ratio of the friction coefficients of the stretched to coiled conformations, i.e., depending on the ratio of the polymer length to the coil size. The values were obtained with high resolution numerically and confirmed experimentally [15]. Dynamical slowing down due to increasing fluctuations of molecular configurations at the onset is similar to the critical slowing down in a continuous phase transition. A similar, albeit much weaker, increase of the relaxation time is encountered in a fast-fluctuating isotropic random flow [16,17].

II. COIL-STRETCH TRANSITION

The current paper is devoted to the coil-stretch transition of polymers in a random flow. Our goal is to introduce the new way to characterize the transition, presented in Fig. 1, and compare it with the previously used way, presented in Fig. 2. Our flow is that of elastic turbulence (ET) [18–20], where polymer fluctuations generated by the flow are far from thermal equilibrium and strongly exceed thermal noise. Flow-stretched polymer chains make fluid elastic. When the elastic energy overcomes the dissipation due to polymer relaxation, an elastic instability takes place for flows with curvilinear trajectories [21,22]. Further increasing Wi, one obtains ET, a

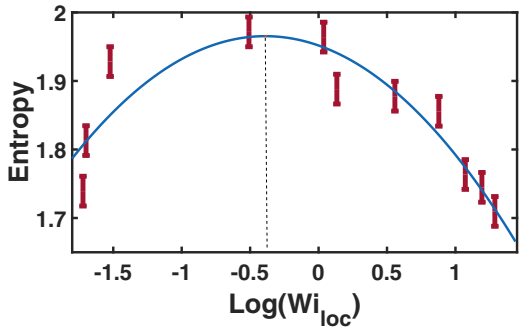

FIG. 1. Dependence of the entropy of polymer extensions on the local Weisenberg number $\mathrm{Wi}_{\mathrm{loc}} = \lambda(\partial V_\theta/\partial r)^{\mathrm{rms}}$ in elastic turbulence. The entropy maximum $S = 1.97 \pm 0.042$ at $\log_2(\mathrm{Wi}_{\mathrm{loc}}) = -0.39 \pm 0.48$ is interpreted as the coil-stretch transition in the interval $0.13 < \mathrm{Wi}_{\mathrm{loc}} < 1.23$.

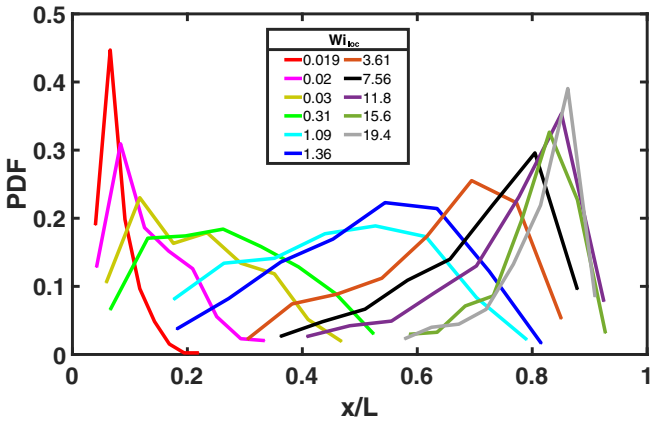

FIG. 3. PDFs of polymer extension, based on the statistics of about 900 molecules for each $\mathrm{Wi}_{\mathrm{loc}}$.

spatially smooth and temporally random flow [18–20], which allows us to study the dynamics and conformation of a single polymer molecule in a random flow at the Reynolds number $\mathrm{Re} \ll 1$ [23]. The existence of the coil-stretch transition in ET has been demonstrated in the single-polymer experiment [24–27] by measuring the probability distribution function (PDF) $P(x/L)$ of the polymer extension x, normalized by the maximal polymer length L, and comparing it with the theory [28,29] and numerical simulations [30], both based on the linear Oldroyd-B polymer model [31].

Below the transition, the theory predicted the power-law PDF tail, $P(x/L) \propto x^{-1-\alpha}$, with a linear dependence of α on $1/\mathrm{Wi}_{\mathrm{loc}}$ below and in the vicinity of the coil-stretch transition [28], which was indeed observed [24–27]. A positive α corresponds to the majority of polymers molecules being in a coiled state, and a negative α is in the case of the majority of polymers being strongly stretched. The condition $\alpha = 0$ is the criterion for the coil-stretch transition. Here $\mathrm{Wi}_{\mathrm{loc}} = \lambda\gamma$

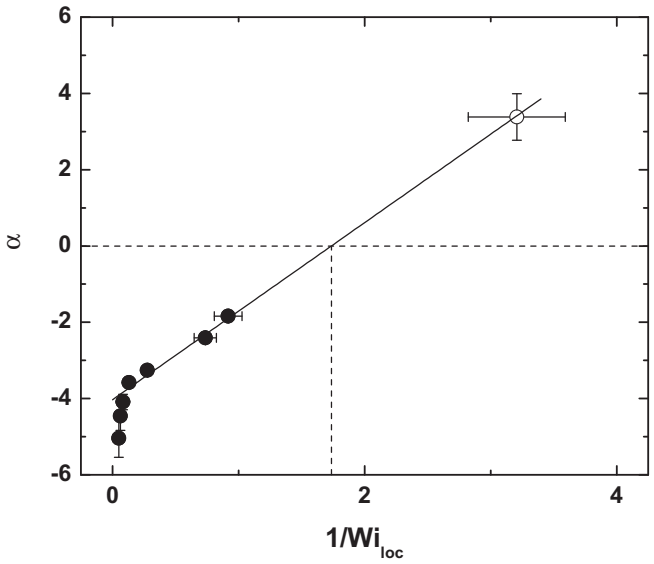

FIG. 2. Determination of the onset of the coil-stretch transition Wi_c using the exponents α of the power-law tail of the PDFs of polymer extensions: $\mathrm{Wi}_{\mathrm{loc}} = 0.58 \pm 0.20$.

with γ either the largest Lyapunov exponent of a random flow or $\gamma \approx (\partial V_\theta/\partial r)^{\mathrm{rms}}$ in an isotropic random flow, where V_θ and r are the azimuthal velocity and radial coordinate, respectively, in the swirling flow [28,29]. Unfortunately, a well-defined tail can be observed only outside of the transition region [24,26,27], as seen also from Fig. 3, so that the vicinity of the critical point cannot be characterized in this way. Indeed, polymer fluctuations are expected to be strong near the transition onset, since the effective polymer free energy has wide minima (corresponding to coiled and stretched conformations) separated by a low barrier, which is comparable with the thermal energy k_BT, yet much smaller than the polymer energy due to velocity fluctuations in ET [14]. Moreover, since polymers are only slightly stretched below the transition, experimental resolution limits the determination of the power-law exponent of the PDF tail. Therefore, most of the data are obtained above the transition, where theory based on the Oldroyd-B model is not applicable [28,29]. Fortunately, the theory based on the FENE model [17] revealed the linear dependence $\alpha \propto \mathrm{Wi}_{\mathrm{loc}}^{-1} - \mathrm{Wi}_{\mathrm{loc},c}^{-1}$ both below and above the transition, where $\mathrm{Wi}_{\mathrm{loc},c}$ is the transition value of $\mathrm{Wi}_{\mathrm{loc}}$.

In Fig. 2, we plot α as a function of $1/\mathrm{Wi}_{\mathrm{loc}}$. At very high $\mathrm{Wi}_{\mathrm{loc}}$ (where elastic turbulence takes place), the dependence $\alpha(1/\mathrm{Wi}_{\mathrm{loc}})$ is nonlinear. It is getting linear closer to the transition. The point to the right (below the transition) is approximately on this line. Therefore, identifying the transition point by drawing a straight line is a meaningful but quite rough procedure, since there is no data in the wide interval $1 < 1/\mathrm{Wi}_{\mathrm{loc}} < 3$. The linear fit to the data intersects with $\alpha = 0$ at the critical value of $\mathrm{Wi}_{\mathrm{loc}} = 0.58 \pm 0.20$, which is close to that theoretically predicted and obtained by the numerical simulations and experiments on λ-DNA [24,28–30,32,33]. The logarithm of the critical value, $\log_2 0.58 = -0.24$ is close to the value -0.39 shown in Fig. 1, even though one should not put too much emphasis on the specific value taken from that broad maximum.

The Fig. 1 presents the new approach, based on the entropy of the extension PDF, which is expected to have a maximum at the transition, as indeed is seen in Fig. 1. While fluctuations are often characterized by a variance, it is a proper measure only for Gaussian distributions, which is definitely not the

case for extension statistics, as can be seen from Fig. 3. On the contrary, entropy is a universal measure of uncertainty. In every case, we divided the interval of possible extensions into $M = 8$ bins and discretized the PDF of the extensions as P_i for $i = 1, \ldots, 8$ with normalization $\sum_i P_i = 1$. The entropy in bits was then computed as $S = -\sum_i P_i \log_2 P_i$. The uncertainly in determining the values of the entropy is due to a finite sample size, so that the probabilities P_i have statistical errors. While those errors are unbiased, there is a systematic error in the entropy, because it is a nonlinear function of probabilities. That error can be estimated as the number of bins M divided by the total number of points $N \simeq 900$; our choice of M guarantees that this error is less 1% . On the other hand, the number of bins cannot be too small, lest we fail to distinguish between different distribution; the number $M = 8$ was chosen to provide maximal entropy variation and minimal systematic error for that interval of Wi. Apart from the systematic error, there is also a much larger statistical error in the entropy values. To determine it and find the maximum position, we approximate the entropy Wi dependence (as any function near a maximum) by a parabola and compute the variance of our data with respect to this curve. This squared deviation is found to be 0.0145, which gives the rms error of the entropy values $\sqrt{0.0145/(11-3)} \approx 0.042$, where 11 is the number of points and 3 is the number of fitting parameters (of the parabola). Because of the parabolic dependence, the uncertainty of determining the position of the maximum in $\log \mathrm{Wi}$ is much larger and equal to $\sqrt{0.042/2(0.09)} \approx 0.48$, where 0.09 is the curvature of the parabola. The position of the maximum in $S(\mathrm{Wi})$ with that accuracy is $\log_2(\mathrm{Wi}_{\mathrm{loc}}) = -0.39 \pm 0.48$, which places the critical point in the interval $0.13 < \mathrm{Wi}_{\mathrm{loc}} < 1.23$. The entropy (in bits) characterizes the level of extension fluctuations at the transition: for the eight-bin distribution, $S \simeq 1.75 \pm 0.042$ bits both far below and above the transition and raises to $S = 1.97 \pm 0.042$ bits at the transition.

It is also instructive to look at the changes of the extension PDF on the increase of the flow gradients, see Fig. 3. Before the coil-stretch transition due to weak polymer stretching and its limited experimental resolution, only a single point in Wi of the right tail slope of PDF with the maximum at the left (Fig. 3) is presented in Fig. 2. After the transition, the maximum does not jump to the polymer maximal extension, but gradually moves there with the left slope increasing. The evolution of the PDF, both before and after the transition, can be understood in terms of the Lagrangian statistics of Lyapunov exponents [28,34].

III. MEASUREMENTS

The rest of the paper describes the measurements. We conducted our experiments using a stock polymer solution of (0.3–0.4) mg/ml T4GT7 (T4)DNA with molecular weight of $M_w = 1.08 \times 10^8$ (165.6 kbp) obtained from Nippon Gene. A T4DNA solution with concentration $c = 25.16\ \mu$g/ml (the overlap concentration $c* = 19.2\ \mu$g/ml) was prepared by diluting the stock solution by the mixed solvent, a pH 8 buffer containing 10 mM Tris-HCl, 2 mM EDTA, 10 mM NaCl, 4% β-mercaptoethanol, glucose oxidase (50 μg/ml), and catalase (10 μg/ml), with saccharose of concentration

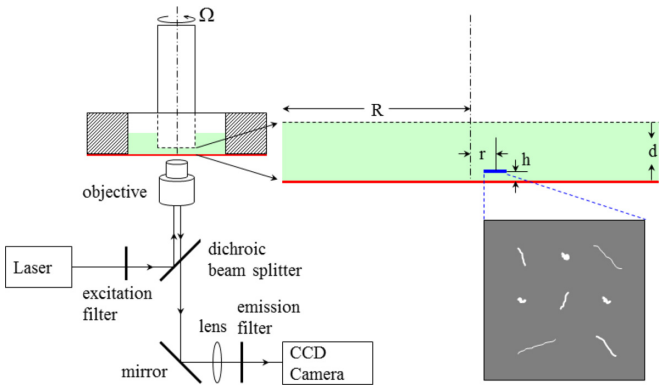

FIG. 4. Experimental setup. A von Karman swirling flow is created in the gap of $d = 675\ \mu$m between the flat end face of the rotating delrin rod of radius $R = 2.25$ mm ($d/R = 0.3$) and a cover slip. The plastic rod is glued into the metal shaft that is driven via a belt by an optically encoded dc minimotor with less than 1% rms of velocity fluctuations. Beating of the polished delrin surface due to misalignment is less than 1 μm on a radius of 300 μm. The delrin-made cell has an inner radius $R_c = 6$ mm.

50% [24–27]. The solvent viscosity was measured to be $\eta_s = 14.7$ cP on the stress-controlled rheometer AR 1000N (TA Instruments).

To study the statistics of polymer extensions in the solution of T4 DNA, the same fluorescently labeled molecules with YOYO-1 (Molecular Probes) at dye-to-basepair ratio of 1:4 is added in concentration 1 ng/ml. At equilibrium, the coiled T4DNA has the gyration radius $R_G \approx 1.5\ \mu$m, while its entire contour length with the intercalated dye molecules is $L \approx 71.7\ \mu$m with roughly 1100 persistence lengths [35,36].

Fluorescently stained T4DNA are imaged using a home-built epifluorescent microscope by a 40×, 1.3 NA oil-immersion objectives (Zeiss) with 0.4 μm depth of focus. The setup is shown in Fig. 4; it is similar to that used in our previous experiments of the coil-stretch transition in λ-DNA in a random flow of a dilute polymer solution [24], where we elucidated the role of a shear strain on the polymer stretching and estimated elastic stress via a force necessary for the stretching [25,26]. The fluorescent dye is excited by a 488-nm argon-ion laser reflecting on a 505-nm long-pass dichroic mirror. Fluorescence emanating from the fluorophore passes through a 515-nm long-pass emission filter before it is recorded with a PhotonMax 512B EMCCD camera (Princeton Instruments) of spatial resolution down to 0.5 μm at 20 or 25 fps. To reduce photo-induced degradation, the molecules are stroboscopically illuminated using a chopper synchronized with the camera. The measurements were carried out on area of $267 \times 267\ \mu\mathrm{m}^2$ at the radial location $r = 300\ \mu$m and $h = 100\ \mu$m above the cover glass at the rotation velocity in the range of $\Omega = 0$-15.7 1/s that corresponds to $\mathrm{Wi} = s\lambda = 0108$, where $s = \Omega r/d$ is the shear rate and d is the gap between the flat end face of the rotating delrin rod and a cover slip. Due to the narrow focal depth, three-dimensional (3D) motion of a molecule can be traced only during its location in 2D imaging plane, and only those molecules remained totally in a focus are analyzed.

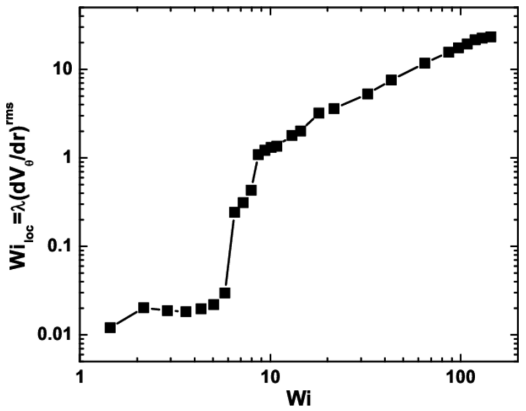

FIG. 5. The dependence of the local Weissenberg $\mathrm{Wi}_{\mathrm{loc}} = \lambda(\partial V_\theta/\partial r)^{\mathrm{rms}}$ on Wi in a swirling flow between two disks.

The longest polymer relaxation time λ is measured by relaxation of stretched single T4DNA molecules in a solution subjected to a shear flow with sufficiently high shear rate. After the flow is abruptly stopped, the conformation of a single molecule is recorded as a function of time. The polymer extension has been measured for each conformation and then averaged over about 20 molecules. The resulting decay of the averaged square of polymer extension $\langle xx\rangle$ is fitted by a single exponential decay in the region of a relative extension less than $0.3-0.4$ by $\langle xx\rangle = A\exp(-t/\lambda) + B$ that provides the longest polymer relaxation time $\lambda = 15.5 \pm 0.3$ s (see Fig. 1 in Ref. [27]). The relaxation times obtained by the square molecule extension relaxation is in a good agreement with those obtained from stress relaxation of the bulk solution by rheometer [37], which shows the inherent correlation between single polymer conformation and its macroscopic solution elasticity [4].

For the analysis we use the data both below and above the coil-stretch transition up to the highest values of Wi. By tracking individual molecules, we measure PDF of the polymer extensions x. For sufficiently large number of molecules analyzed (about 900 for each Wi), the statistics is representative for all molecules in a 3D random flow. The structure and fluctuations of velocity and velocity gradient fields in 3D are characterized by using particle image velocimetry (PIV) measurements. The fluorescent particles with diameter of 0.5 μm at a concentration of 500 ppm are added to polymer solutions as seeding particles to carry out PIV measurements.

The theory suggests that the coil-stretch transition of polymer in a random flow is characterized by the transformation of the PDF of molecular extension as a function of $\mathrm{Wi}_{\mathrm{loc}}$. The values of the rms fluctuations of the velocity gradients, $(\partial V_\theta/\partial r)^{\mathrm{rms}}$, were obtained by the PIV measurements in the same polymer solution at different Wi that is shown in Fig. 5.

To obtain the probability distributions (PDF), the molecular extension in a polymer solution of $c = 25.16$ μg/ml with 50% sucrose were measured at different Wi below and above the elastic instability threshold $\mathrm{Wi}_c = 5.8$. Figure 6 shows the PDF of the relative polymer extension x/L in a wide range of Wi values from 2.9 and up to 108. At $\mathrm{Wi} = 7.2$, T4DNA molecules are weakly stretched with majority of the molecules in the coiled state, and a positive $\alpha = 3.4$ is found. At $\mathrm{Wi} = 8.7$ close to the coil-stretch transition, the PDF has a broad distribution and α approaches 0. At $\mathrm{Wi} = 108$, T4DNA molecules are strongly stretched with a negative $\alpha = -5.0$ (see Fig. 6). The linear dependence of α on $1/\mathrm{Wi}_{\mathrm{loc}}$ below the critical value of $\mathrm{Wi}_{\mathrm{loc}}$ and above it at moderate polymer stretching $R_G/L \ll x/L \ll 1$ breaks down at $x \simeq L$. On the other hand, the theory based on the FENE model shows the opposite tendency: the linear dependence of α on $1/\mathrm{Wi}_{\mathrm{loc}}$ above $\mathrm{Wi}_{\mathrm{loc},c}$ at moderate polymer stretching decreases and reaches the asymptotic value $\alpha = -2$. This evident qualitative discrepancy with the experimental data is corrected in the recent theory by taking into account internal friction as an important factor in polymer stretching statistics. It leads to a quantitative agreement with the experiment [38].

To summarize, we studied the dynamics and conformations of single, stained fluorescently T4DNA molecules in a random flow of elastic turbulence created by the same unlabeled molecules. We introduced the new experimental method to determine and quantify the coil-stretch transition and compared such characterization with the traditional approach based on the theories using either linear Oldroyd-B or nonlinear FENE polymer models. The methods agree in identifying the transition within their statistical uncertainty intervals. With the existing ..statistics ($N \simeq 900$ in every histogram), the entropic method gives wider uncertainty, yet it has the advantage of being purely empirical and independent of theoretical assumptions. In addition, the entropic method can characterize the level of fluctuations at the transition, showing in our case

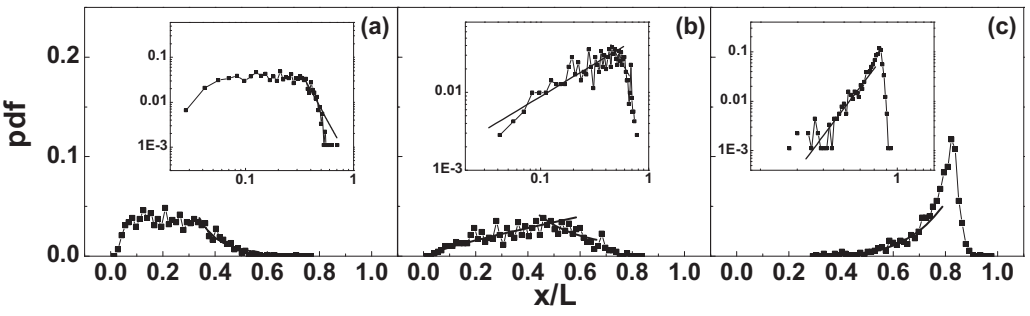

FIG. 6. [(a)–(c)] PDFs of the T4DNA normalized stretching in linear-linear presentation in the main plots and in log-log presentation in the corresponding insets at $\mathrm{Wi} = 7.2$ (a), 8.7 (b), and 108 (c) in a solution of $c = 25.16$ μg/ml with 50% sucrose. The thick solid lines are algebraic fittings to the PDF tails $P(x/L) \sim (x/L)^{-1-\alpha}$ with $\alpha = 3.4$ at $\mathrm{Wi} = 7.2$, $\alpha = -1.8$ (left tail) at $\mathrm{Wi} = 8.7$, and $\alpha = -5.0$ at $\mathrm{Wi} = 108$.

that the entropy increases from 1.75 to 1.97 bits, which is substantial.

The work was supported by the Excellence Center at WIS, the Simons Grant No. 662962, Grant No. 075-15-2019-1893 by the Russian Ministry of Science, Grants No. 873028 and No. 823937 of the EU Horizon 2020 program, Grant No. 882/19 of Israel Science Foundation, Grant No. 2016145 of Binational USA-Israel Science Foundation, and Grant No. Y928021001 of the Chinese Academy of Sciences.

[1] R. G. Larson, *Constitutive Equations for Polymer Melts and Solutions* (Butterworths, Boston, 1988).
[2] P. G. de Gennes, J. Chem. Phys. **60**, 5030 (1974).
[3] E. J. Hinch, in *Proceedings of Colloques Internationaux du CNRS No. 233* (CNRS Editions, Paris, 1974), p. 241.
[4] T. Perkins, D. Smith, and S. Chu, Science, **276**, 2016 (1997).
[5] R. G. Larson, H. Hu, D. E. Smith, and S. Chu, J. Rheol. **43**, 267 (1999).
[6] P. G. de Gennes, Science **276**, 1999 (1997).
[7] D. E. Smith and S. Chu, Science **281**, 1335 (1998).
[8] J. S. Hur, E. S. G. Shaqfeh, H. P. Babcock, and S. Chu, Phys. Rev. E **66**, 011915 (2002).
[9] H. P. Babcock, R. E. Teixeira, J. S. Hur, E. S. G. Shaqfeh, and S. Chu, Macromolecules **36**, 4544 (2003).
[10] Ch. M. Schroeder, H. P. Babcock, E. S. G. Shaqfeh, and S. Chu, Science **301**, 1515 (2003).
[11] Ch. M. Schroeder, E. S. G. Shaqfeh, and S. Chu, Macromolecules **37**, 9242 (2004).
[12] C. C. Hsieh and R. G. Larson, J. Rheol. **49**, 1081 (2005).
[13] D. Vincenzi and E. Bodenschatz, J. Phys. A: Math. Gen. **39**, 10691 (2006).
[14] A. Celani, A. Puliafito, and D. Vincenzi, Phys. Rev. Lett. **97**, 118301 (2006).
[15] S. Gerashchenko and V. Steinberg, Phys. Rev. E **78**, 040801(R) (2008).
[16] A. Celani, S. Musacchio, and D. Vincenzi, J. Stat. Phys. **118**, 531 (2005).
[17] M. Martin Afonso, D. Vincenzi, J. Fluid. Mech. **540**, 99-108 (2005).
[18] A. Groisman and V. Steinberg, Nature (London) **405**, 53 (2000).
[19] A. Groisman, V. Steinberg, Nature (London) **410**, 905 (2001).
[20] A. Groisman and V. Steinberg, New J. Phys. **6**, 29 (2004).
[21] R. G. Larson, Rheol. Acta **31**, 213 (1992).
[22] E. S. G. Shaqfeh, Annu. Rev. Fluid Mech. **28**, 129 (1996).
[23] A. Groisman and V. Steinberg, Phys. Rev. Lett. **86**, 934 (2001).
[24] S. Geraschenko, C. Chevallard, and V. Steinberg, Europhys. Lett. **71**, 221 (2005).
[25] Y. Liu and V. Steinberg, Europhys. Lett. **90**, 44002 (2010).
[26] Y. Liu and V. Steinberg, Europhys. Lett. **90**, 44005 (2010).
[27] Y. Liu and V. Steinberg, Macromol. Symp. **337**, 34 (2014).
[28] E. Balkovsky, A. Fouxon, and V. Lebedev, Phys. Rev. Lett. **84**, 4765 (2000).
[29] M. Chertkov, Phys. Rev. Lett. **84**, 4761 (2000).
[30] B. Eckhardt, J. Kronjager, and J. Schumacher, Comput. Phys. Commun. **147**, 538 (2002).
[31] R. B. Bird and O. Hassager, *Dynamics of Polymeric Liquids: Fluid Mechanics*, 2nd ed. (Wiley, New York, 1987).
[32] P. A. Stone and M. D. Graham, Phys. Fluids **15**, 1247 (2003).
[33] T. Watanabe and T. Gotoh, Phys. Rev. E. **81**, 066301 (2010).
[34] G. Falkovich, K. Gawedzki, and M. Vergassola, Particles and fields in turbulence, Rev. Mod. Phys. **73**, 913 (2001)
[35] D. E. Smith, T. T. Perkins, and S. Chu, Macromolecules **29**, 1372 (1996).
[36] R. M. Robertson, S. Laib, and D. E. Smith, Proc. Natl. Acad. Sci. USA **103**, 7310 (2006).
[37] Y. Liu, Y. Jun, and V. Steinberg, J. Rheol. **53**, 1069 (2009).
[38] D. Vincenzi (private communication).